AIAA JOURNAL
Vol. 36, No. 6, June 1998

Exponentially Accelerating Jet in Crossflow

Adnan Eroglu* and Robert E. Breidenthal†
University of Washington, Seattle, Washington 98195

Effects of exponential acceleration on penetration and mixing characteristics of a jet in crossflow have been investigated experimentally in a water model. To impose an exponential acceleration on the flow, both the injection speed and the nozzle width of the jet increased exponentially in the downstream direction of the crossflow. An acceleration parameter α is defined as the ratio of the revolution time of the longitudinal vortex pair to the *e*-folding time of the acceleration. Theoretically, a significant reduction in turbulent entrainment and mixing of the jet with the crossflow is expected as α nears unity or as the revolution time of the longitudinal vortex pair in the jet becomes comparable to the characteristic time of acceleration. It was found that the diameter of each vortex in the near-field jet cross section is reduced more than a factor of three as α is increased from 0 to 2.5. In the same α range, the jet flame or reaction length increased up to 50%, revealing a strong effect of the near-field forcing on the far-field molecular scale mixing. Furthermore, the experiments have shown up to a 50% increase in the penetration of the jet into the crossflow as a result of the acceleration, when compared with a conventional transverse jet. These results demonstrate clearly that, in a free-shear flow, imposing a new timescale by means of an external acceleration influences the entrainment and mixing characteristics dramatically, thus providing a new possibility of controlling the flow characteristics.

Nomenclature

d = hydraulic diameter
d_j = nozzle width at any x
d_0 = nozzle width at x equals 0
R = jet-to-freestream-velocity ratio
Re = Reynolds number
s = center-to-center vortex spacing
t = time
t_e = e-folding time of the exponential acceleration function
t_n = nozzle time
V_j = jet velocity at any x
V_0 = jet velocity at x equals 0
V_∞ = uniform crossflow speed
x = streamwise coordinate
x_e = e-folding distance of the exponential acceleration function
x_f = flame or reaction length
α = acceleration parameter
δ = vortex size
ϕ = stoichiometric ratio

I. Introduction

THE recognition of the large-scale coherent structures and their role in turbulent mixing in the early 1970s paved the way for a variety of studies on free-shear flows with external forcing. It has been demonstrated for a number of cases that large-scale vortical structures can be forced externally, such that interaction among discrete vortices can be controlled to reduce or enhance mixing. Among the various flows related to this, the forced shear layer,[1,2] pulsed freejet,[3] and pulsed transverse jet[4] can be cited. In all of these investigations, it was observed that imposing an external timescale on the interaction process of large-scale vortices changes the average flow properties, such as the growth rate of a shear layer (or a jet) and the penetration depth of a transverse jet.

The primary goal of the work reported here can be related to the work just cited, namely, altering the nonsteady interaction among the organized vortical structures by external forcing. However, the approach taken in the present work is significantly different and relies mainly on controlling the turnover time and the strength of the vortices rather than their formation frequency.

This approach is based on a recent theoretical notion that suggests a significant change in the entrainment behavior of large-scale vortices under suitable temporal or spatial accelerations,[5,6] e.g., an exponential acceleration function with e-folding time comparable to the rotation period of the large-scale vortices. According to this thinking, it would be possible to control the entrainment carried out by large-scale vortices, provided that this acceleration requirement is satisfied.

Although the concept of utilizing an external acceleration or forcing to control large-scale turbulent mixing is potentially applicable to numerous free-shear-flow cases, this study has mainly concentrated on controlling the interaction of a jet with a uniform crossflow, with practical interest in mixing of a fuel jet with a transverse airstream.

For a conventional transverse jet, the injected fluid becomes progressively more dilute as it moves away from the nozzle, and so all local mixture ratios are eventually achieved. However, for applications such as combustion and chemical reaction processes, it is desirable to control the mixing so that the reaction takes place at the optimum local mixture ratio, e.g., locally fuel-lean conditions for reduction of NO_x formation. Moreover, for a fuel jet introduced into a uniform crossflow, isolating the injection process from mixing is desirable to provide better penetration of the fuel into the cross stream and to inhibit the combustion instabilities associated with the near field of the injection. For example, in the case of hypersonic combustion, it is preferred to have the fuel jets penetrating through the hot boundary layer without significant mixing and only after reaching the cooler freestream flow to mix and burn rapidly.

The earliest experimental work aimed at testing the influence of the acceleration concept just mentioned was conducted by Kato et al.[7] with a free round jet of constant diameter but with time-dependent injection velocity. Their results indicated about a 25% increase in flame or reaction length over an equivalent steady jet when the injection velocity increased linearly in time, as measured with a chemical reaction in water. Preliminary experiments with a freejet have demonstrated a dramatic reduction in the growth rate of the jet (about 36% reduction in the spreading angle of the jet) when both the jet injection area and speed increase exponentially in time. The experiments conducted by Clement and Rodriguez[8] in a supersonic tunnel with an array of discrete sonic jets of exponentially increasing diameter demonstrated a much weaker bow shock ahead of the injection location compared with a single jet of equal momentum flux. Although they observed a nearly uniform jet fluid

Received July 16, 1997; revision received Jan. 12, 1998; accepted for publication Jan. 19, 1998.

*Research Assistant, Department of Aeronautics and Astronautics; currently Project Leader, Department of Aerodynamics and Combustion, ABB Corporate Research, Ltd., CH5405 Baden-Daettwil, Switzerland.

†Professor, Department of Aeronautics and Astronautics. Member AIAA.

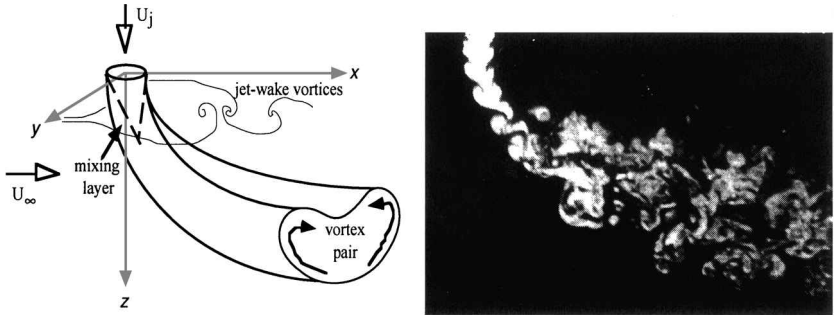

Fig. 1 Sketch and an internal, streamwise LIF picture of the round turbulent jet in a crossflow.

concentration in the near field of the injection, the supersonic flow conditions and the visualization technique they used did not allow a detailed analysis of the jet structure.[8]

A fully exponential transverse jet has been investigated through water model experiments, where both injection speed and size increase exponentially in the crossflow direction. The resulting flow was studied relying extensively on flow visualization techniques such as inert dye injection and laser-induced fluorescence (LIF). Molecular-scale mixing was analyzed by utilizing an acid–base reaction without any heat release and finite chemical rate effects. Employing water as the working fluid has proved to be an extremely powerful technique for a detailed analysis of the flow and the evolution of main vortical structures.

II. Round Steady Jet

Because of its numerous practical applications, ranging from combustion and thrust control to environmental disposal of effluents into the atmosphere and water, the jet in a crossflow has been studied for several decades. A commonly observed view of this flow is presented in Fig. 1 with a sketch of the primary vortical structures and a picture of the side view of the flow.

The prominent feature of the flowfield is that the jet fluid is deflected in the direction of the crossflow as its cross section quickly assumes a kidney shape, dominated by a pair of counter-rotating vortices. A mixing layer develops on the periphery of the jet as the potential core of the jet ends as a cone, slightly bent in the direction of the crossflow. It has been explicitly stated[9–11] or implied in the literature that the entrainment into the jet is mainly due to the counter-rotating vortex pair, observed in the cross section of the jet. Consequently, a significant portion of the earlier research has concentrated mainly on the structure of the jet cross section, either measuring,[9,10,12,13] theoretically modeling,[14–16] or computing[17–19] the strength and spacing of the vortex pair.

This research was also based on the assumption that the longitudinal vortex pair is the primary structure for large-scale entrainment in a transverse jet. Consequently, an acceleration scheme was adapted to affect mainly this vortex pair by means of an acceleration function applied along the injection region. In the following section, the considerations in the selection of this near-field acceleration and its potential impact on the far-field mixing will be explained.

III. Vorticity Dynamics with Exponential Acceleration

The theory behind the exponential acceleration scheme[5,6] can be summarized as follows. For all unforced self-similar flows, the global vorticity of each vortex decays inversely proportional to its own Lagrangian age. This can be verified on the grounds of dimensional analysis inasmuch as the age of the vortex is the only timescale entering the problem.

Physically, dilution of vorticity is mainly due to incorporation of the irrotational ambient fluid into the vortex. A vortex of size δ (meters) and circulation Γ (square meters per second) has a volume flow rate engulfment appetite of order $\delta\Gamma$. To satisfy this appetite, a vortex formed at the near field, a free jet, for example, engulfs both the ambient fluid and the jet fluid injected at a later instant as it moves downstream.

It is proposed that imposing a new timescale on the flow would alter the aging characteristics of the vortices. If the submerged jet fluid is accelerated as it exits from the nozzle with an acceleration

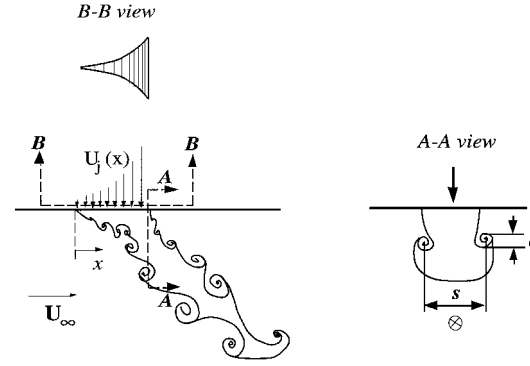

Fig. 2 Exponential jet in a crossflow; streamwise and transverse cross sections.

function that has a time constant t_a, then it is plausible to expect a vortex to preferentially engulf the rotational jet fluid injected at a later time, rather than the ambient fluid, because the acceleration would place the newly injected fluid at the back side of the vortex, the observed location of large-scale entrainment.[20,21] Therefore, entrainment of the ambient fluid into each vortex would be controlled by the externally applied acceleration conditions.

Engulfment by a vortex requires about a full vortex rotation.[22,23] This implies, for the case of the acceleration time constant being equal to the turnover time of the vortices, that there would be little entrainment of the ambient fluid into the vortices because the engulfment appetite of each vortex is predominantly satisfied by the accelerating jet fluid. This corresponds to the case of little mixing of the jet fluid with the ambient fluid during the acceleration.

Implementation of this concept is carried out here by replacing the time coordinate with a spatial one. Namely, in these experiments the jet diameter and the injection speed do not vary in time but both increase exponentially with downstream distance as shown in Fig. 2, i.e.,

$$d_j(x) = d_0 e^{x/x_e} \tag{1}$$

$$V_j(x) = V_0 e^{x/x_e} \tag{2}$$

The spatial nonsteadiness is brought into the problem by introducing this jet into a crossflow. Then, as a crossflow fluid element moves along the accelerating injection region, it feels an exponentially increasing impulse due to the jet fluid. The characteristic timescale associated with the revolution of each vortex in the vortex pair that is formed along the injection can be expressed as the ratio of the local injection width to the local injection speed:

$$t_n = \frac{d_j(x)}{V_j(x)} \tag{3}$$

which is called the local nozzle time.

Substituting Eqs. (1) and (2) into Eq. (3),

$$t_n = d_0/V_0 \tag{4}$$

yields a constant t_n along the injection length.

Imposing an acceleration on the flow introduces a new timescale. Because the acceleration function is exponential, this characteristic

timescale is the e-folding time of this function t_e, which can be defined as

$$t_e = x_e / V_\infty \tag{5}$$

The significance of t_e is that, as a fluid element is convected downstream past the nozzle array with a speed of approximately V_∞, it is subjected to an e-fold increase in the impulse on it from the jet during this time period.

An acceleration parameter can be defined as the ratio of these two timescales:

$$\alpha = t_n / t_e = d_0 V_\infty / x_e V_0 \tag{6}$$

Theoretically, one should expect a significant change in the structure of the vortex pair when $\alpha \cong 1$ because the vortex pair would make about one revolution by the time it experiences an e-fold increase in acceleration. In other words, the rotation time of the vortex pair would be matched with the convection time of it along a distance where a significant change in acceleration occurs. From the entrainment point of view, matching these two timescales along the injection length means that newly injected fluid is placed on the lee side of the previously injected part of the jet at a rate such that it can properly fulfill the engulfment appetite of the vortex pair it forms as it is convected downstream.

IV. Experimental Facility

The facilities used include a water tunnel, two exponential nozzle arrays, a pressurized fluid supply system, a 5-W argon-ion laser, and optical components required for the LIF experiments.

A. Water Tunnel

The experiments were conducted in a horizontal-type recirculating water-tunnel facility with a test section 3 m long and 70×70 cm square cross section. Test section flow speed was varied from 0 to 70 cm/s by changing the frequency input of a 22.4-kW ac motor driving a centrifugal pump. The freestream turbulence intensity in the test section was measured by using a hot-film sensor operated at constant temperature mode and found to be less than 0.3% of the mean flow.

The water tunnel, based on a previous design of Gharib,[24] was constructed of stainless steel, tempered glass, and polyvinylchloride, therefore permitting the use of strong chemical solutions necessary for the flame or reaction length measurements. A contraction section with an inlet-to-exit-area ratio of four and matched-cubic contraction geometry has been employed upstream of the test section for minimum boundary-layer thickness and turbulence intensity in the test section. The two side and bottom walls of the test section are made of single-piece, tempered-glass panels for a full 3-m view from all directions.

B. Nozzle Arrays

The experiments reported here have been carried out with an array of nozzles aligned in the streamwise direction and packed closely together to obtain a stepwise-exponential increase in both injection width and velocity. This nozzle array was made of five individual nozzles, together with a total injection length of 9 cm. The e-folding distance of the exponential profile selected is 3 cm; thus, the array covers a total of three e-folding distances. Each nozzle in the array consists of a combination of flow conditioning devices including a foam straightener, a perforated plate, a wire screen, and a fifth-order polynomial contraction. Adjacent nozzles in the array are separated from each other by 0.05-cm-thick, stainless-steel plates.

The equivalent flow speed for each nozzle in the array was calculated by dividing the integral of the exponential flow rate variation over the nozzle exit section by the nozzle exit area, i.e.,

$$(V_j)_i = \frac{\int_{x_i}^{x_{i+1}} V_j(x) d_0 e^{x/x_e}\, \mathrm{d}x}{\int_{x_i}^{x_{i+1}} d_0 e^{x/x_e}\, \mathrm{d}x}$$

This nozzle array was tested at two different flow speed conditions, referred to as B-1 and B-2, sweeping an acceleration parameter range of $0.25 \le \alpha \le 2.0$ and $0.25 \le \alpha \le 3.0$, respectively. The acceleration parameter was varied by changing the crossflow speed as the jet conditions were held constant at a specific setting.

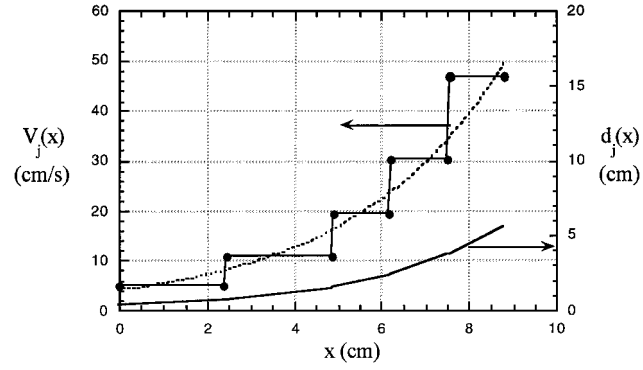

Nozzle array B-1

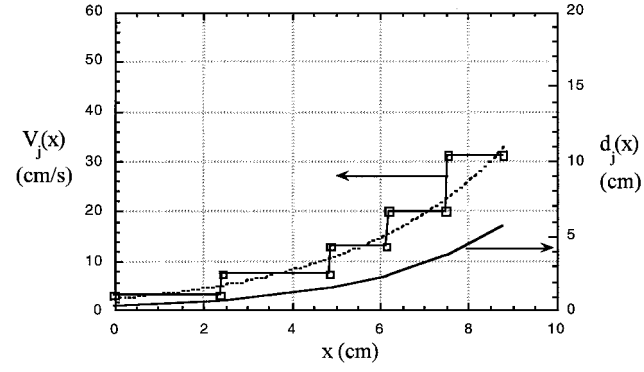

Nozzle array B-2

Fig. 3 Injection velocity and width variation.

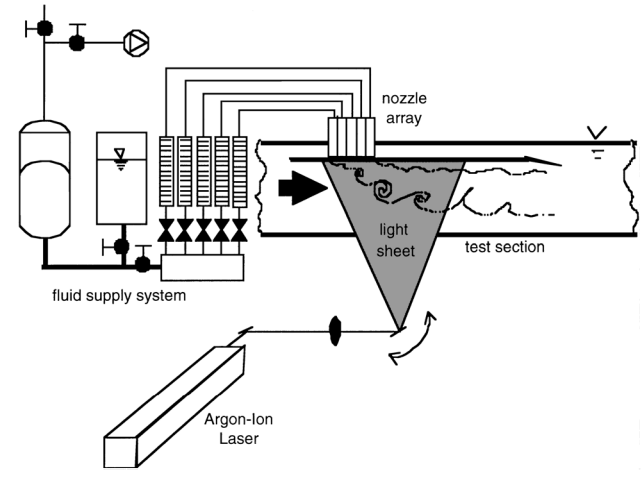

Fig. 4 Fluid supply system and LIF setup.

The variation of the injection speed and the injection velocity along the injection length is given in Fig. 3 for the nozzles used. The lower limit of the acceleration parameter for each nozzle speed setting was chosen to minimize the effect of the bottom wall of the test section on the flow by restricting the jet penetration to a certain depth during the experiments. The maximum speed of the water tunnel defined the upper limit of the acceleration parameter.

The exponential nozzle arrays were machined from clear Plexiglas® and installed on a flat plate with an elliptical leading edge and an adjustable flap at the trailing edge. This plate, installed 15 cm below the water free surface, acted as a false wall with adjustable boundary-layer thickness. The velocity thickness of the crossflow boundary layer at the point of injection is estimated to be about 0.2 mm with this arrangement.

C. Fluid Supply System

A pressurized-air-driven system was used to supply each nozzle in the jet array with the constant volume flow rate necessary to make up the exponential transverse jet. The main components of this setup are shown in Fig. 4. The fluid to be injected is filled in the preparation

tank from the tunnel to prevent any temperature differences and the resulting buoyancy effects between the primary and secondary flows. A vacuum pump was used to transfer the solution from the preparation tank into a pressure vessel by evacuating the air above a rubber diaphragm, which divides this vessel into two parts, the lower part holding the fluid to be injected and the upper part holding the driving air. During a run, the driving pressure above the rubber diaphragm was held at 6.4 atm for all experiments. The exit of the pressure vessel was connected to a distribution manifold with 10 outlets, each in turn connected to a precision regulating valve, a flow meter, and one of the nozzles in the jet array.

D. LIF System

A 5-W argon-ion laser was used for illumination of the internal slices of the flowfield using the LIF technique. The laser beam was passed through a collimating lens and reflected into the test section, as a sheet approximately 1 mm thick, by a mirror oscillating at 1200 Hz. The LIF setup, illuminating a streamwise cross section of the flow, is as shown in Fig. 4. The orientation of the illuminated plane was varied by rearranging this basic setup, using additional mirrors. During the observation of transverse cross sections of the jet, the optical components were mounted on a traversing mechanism to move the laser sheet in a downstream direction to observe the structure of the counter-rotating vortex pair at different stations.

V. Flow Visualization Techniques

The overall features of the jet plume as well as internal slices of the vortical structures were observed by using several techniques, all with the versatile dye disodium fluorescein. The first technique used this dye as an inert scalar in the jet fluid and visualized the flowfield either by diffuse background illumination or by spotlights positioned such that the interface can be best observed via shadow effects. By selecting a high concentration of disodium fluorescein for jet fluid, an opaque jet–crossflow interface has been obtained, permitting visualization of the jet structure.

The second technique used the fluorescing property of this dye in LIF, in which the dyed jet fluid was illuminated with a sheet of laser light. The cross-sectional views of the jet perpendicular to the crossflow direction were observed by using a submerged mirror placed close to the downstream end of the test section to prevent disturbing the flow in the region studied.

The third method consisted of observing the transition of a pH indicator (phenolphthalein) triggered by an acid–base reaction between the jet and the crossflow fluids. Sulfuric acid (H_2SO_4) and sodium hydroxide (NaOH) water solutions were used in each stream. Upon mixing of the two streams at a prescribed volumetric ratio, the purple color of the pH indicator in the jet fluid was turned either on or off, revealing the location where the mixing at this ratio takes place. This ratio is referred to as stoichiometric ratio ϕ, and the visible length of the jet fluid is the flame or reaction length.

A 35-mm, single-lens reflex camera was used for the pictures presented here. The vortex size and flame or reaction length measurements were made from the video recordings of the flowfield. The camcorder used permitted taking pictures at 30 frames/s with a shutter speed of $\frac{1}{1000}$ s. The recordings taken with a zoom lens were further enlarged by a digital video cassette recorder (VCR) on a large screen monitor up to 20 times the original size, thus enhancing the accuracy of the vortex size, penetration, and mixing-length measurements. A consistent averaging method with 10 pictures per plane was used to measure the fluctuating quantities throughout the experiments.

VI. Results and Discussion

A. Flow Structure

Some of the most prominent features of the exponential transverse jet have been observed through spotlight illumination of the jet flow. A sample streamwise-external view of the jet is given in Fig. 5. Evaluation of recordings similar to this picture reveal that near-field penetration of the jet increases exponentially throughout the injection region, similar to the velocity and area variation. The mean penetration depth, when normalized by the local injection width of the jet, was found to be constant along the streamwise injection length of the jet, indicating a self-similar structure. After

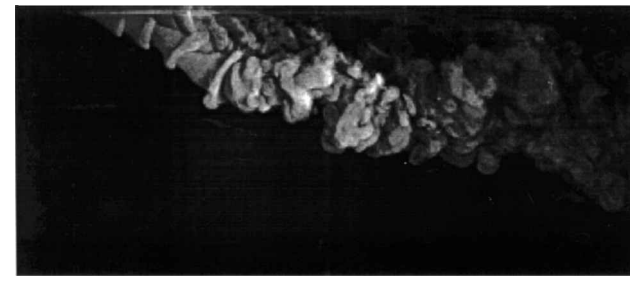

Streamwise view

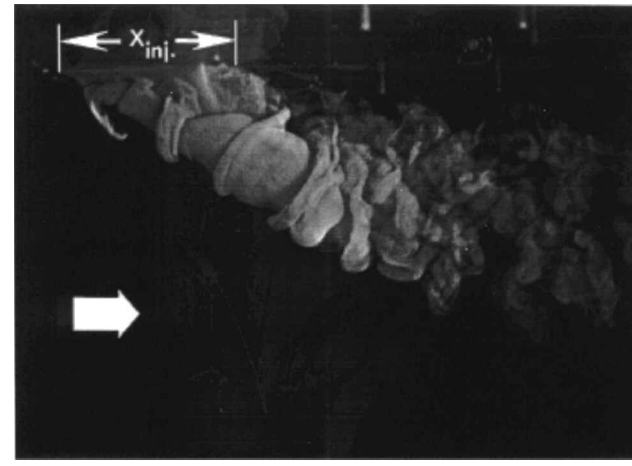

Streamwise, close-up view

Fig. 5 Exponential jet B-2 at $\alpha = 1.0$.

the injection is over, the jet fluid is deflected in the crossflow or downstream direction, as in the case of a conventional transverse jet.

A curved shear layer develops into discrete ring vortices around the jet fluid. One distinct feature of these ring vortices is that the sign of the vorticity undergoes a change at some point along the injection, the exact location depending on the jet-to-crossflow velocity ratio. The vortex rings formed at the interface initially rotate in a counterclockwise direction for almost all velocity ratios because the early part of the jet is much slower than the crossflow. However, farther downstream the newly formed vortices rotate in the clockwise direction as the jet speed increases beyond the crossflow speed.

The transition from one sign of vorticity to the other occurs in the form of a pairing, which takes place in an alternating manner. In other words, if the upstream vortex ring (rotating counterclockwise) comes into interaction with the downstream ring (rotating clockwise) from the left side of it, the pair rapidly propagates upward as a result of their self-induced velocity. On the other hand, if the pairing takes place on the right side of the clockwise-rotating downstream vortex ring, then the pair propagates downward into the crossflow. In both cases the weaker upstream vortex is ultimately incorporated in the stronger downstream one, forming a single vortex ring rotating in the clockwise direction.

The size of the shear layer ring vortices increases in the downstream direction as they entrain the crossflow fluid. However, partly due to the pairing process just mentioned reducing the vortex strength and partly due to the favorable pressure gradient imposed on the freestream due to the exponential jet penetration profile, their growth rate was found to be suppressed along the injection length compared with a conventional single jet in a crossflow.

Using the LIF technique described earlier, with the laser sheet placed perpendicular to the crossflow direction at some point along the injection region, cross-sectional views of the jet are visualized, as shown in Fig. 6. The formation of a pair of counter-rotating vortices, giving a mushroom shape to this cross section, can be observed. As the main emphasis has been placed on studying the response of this vortex pair to acceleration, a significant effort was made to measure their size and spacing as a function of the acceleration parameter α. It was observed that, although the jet cross section

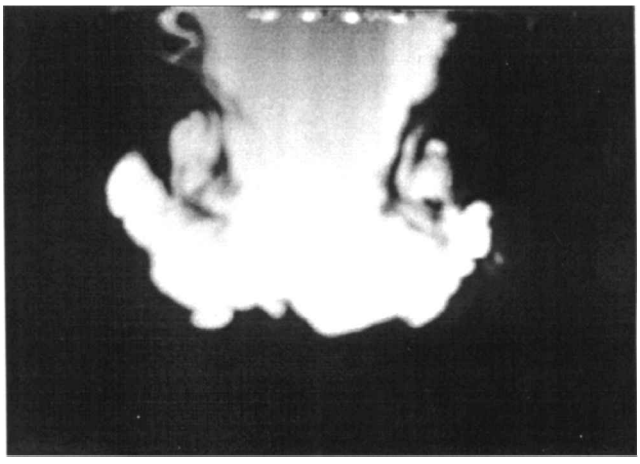

α = 0.25

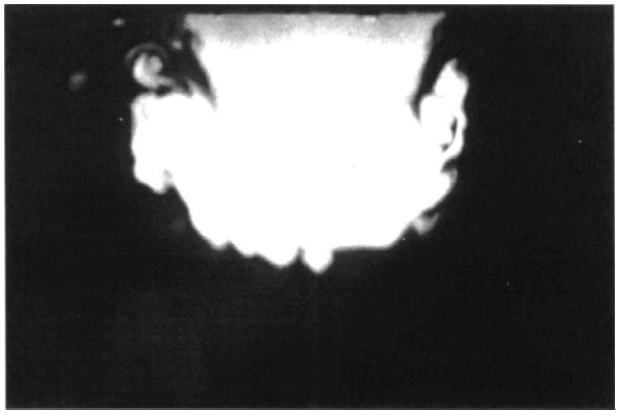

α = 1.0

Fig. 6 Internal, transverse cross sections of the exponential jet B-2.

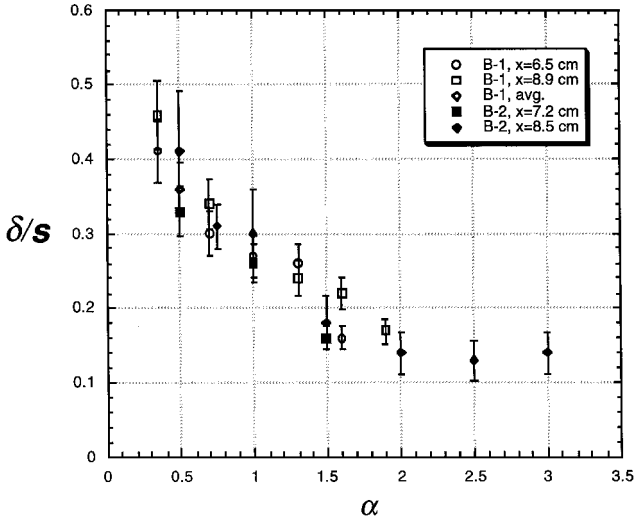

Fig. 7 Normalized vortex size variation with α.

maintains its mushroom shape, its size fluctuates in time as the ring vortices formed around the jet pass through the observation plane at a certain frequency. Because these ring vortices extend to envelop the longitudinal vortex pair, their passage also causes the size of this vortex pair to fluctuate in time. A consistent averaging technique was employed for the results reported, by calculating the average values from the size measured from 10 still pictures for each plane.

A series of experiments measured the size and spacing variation of the counter-rotating vortex pair within the acceleration parameter range of $0.25 \leq \alpha \leq 3.0$. The measured size of these vortices δ normalized by their center-to-center spacing s is given in Fig. 7. A similar behavior was observed for all nozzle arrays tested. That is, the vortices first got significantly smaller in size as α was increased. But δ/s reached an asymptotic value at approximately $\alpha = 2.0$, and no significant change in the size of the vortices was observed beyond this point. However, in this range of α, the rollup process for the initial formation of the vortex pair itself is intermittent. Namely, the fluctuations in the size of the vortices, observed in the lower α region, are replaced by the periodic disappearance of the full structure.

Apparently, independent of the acceleration parameter, when the jet-to-crossflow-velocity ratio R drops below a certain value, the features associated with a transverse jet tend to disappear. In other words, instead of a characteristic counter-rotating vortex pair, the flow is dominated by the shear layer and the wake vortices when R is less than about 1. For the overall velocity ratio settings used in these experiments, this corresponds to the region where α is greater than 2. Thus, it is not surprising to observe that the vortex size is insensitive to the acceleration parameter in this range.

B. Flame or Reaction Length

The mixing structure observed by using an acid–base reaction coupled with the LIF technique reveals that the first place where the jet fluid mixes fully with the crossflow for a given stoichiometric ratio is located on the leeside of the jet. The last place where the final parcel of unmixed jet fluid can be observed is always at the upstream side of the jet. Furthermore, the visible location of the jet tip undergoes periodic fluctuations, and fluctuation length increases with increasing total flame or reaction length. This is analogous to the fluctuations observed in the flame or reaction length of a freejet or thermal, associated with the large-scale structures.[20,21]

The flame or reaction length of the exponential jets B-1 and B-2 were measured at two different stoichiometric ratios; the results are given in Fig. 8. A significant increase is observed in the flame or reaction length as α nears unity. However, increasing α after this point causes the flame or reaction length to decrease back to nearly its unforced value.

The flame or reaction length of a round steady jet was measured for the velocity ratio range of $0.12 < 1/R = V_\infty/V_j < 0.6$ to compare it to that of the exponential jet, and the results are given in Fig. 9. These measurements and similar experiments by Broadwell and Breidenthal[15] have demonstrated that, for a conventional round jet in a crossflow, the flame or reaction length is insensitive to the variations in the crossflow-to-jet velocity ratio, provided that this velocity ratio is above approximately 0.5. For the exponential transverse jet case, the average crossflow-to-jet-velocity-ratio range is $0.5 < 1/R < 3.0$. However, the flame or reaction length varied with increasing velocity ratio even though all of the measurements were made above $1/R = 0.5$.

At low values of α, the increase in the flame or reaction length in Fig. 8 can be attributed to the decrease in the size of the vortex pair observed for the same α range. On the other hand, at larger values

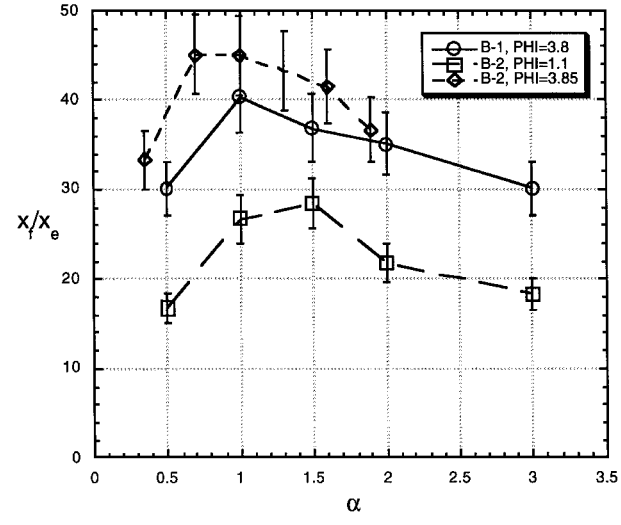

Fig. 8 Normalized flame length variation with α.

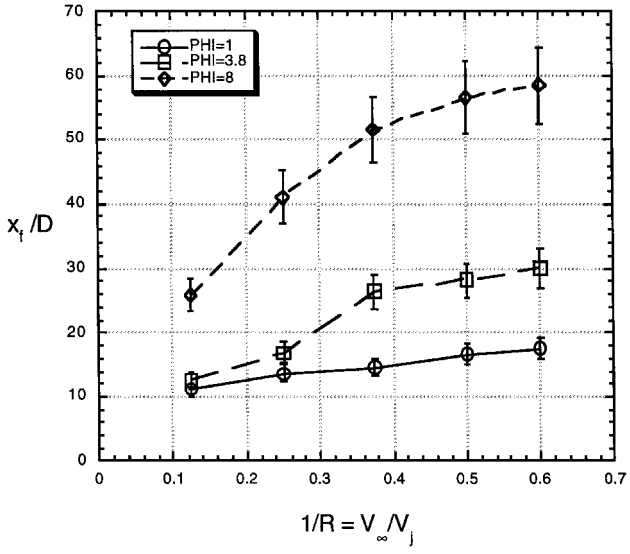

Fig. 9 Normalized flame length variation with 1/*R* for a steady round jet.

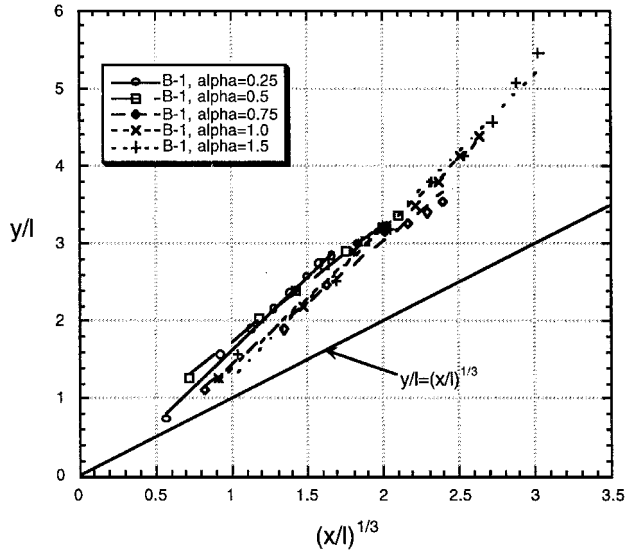

Fig. 10 Normalized penetration variation with downstream distance for the expoenential jet B-1 at different acceleration parameter values.

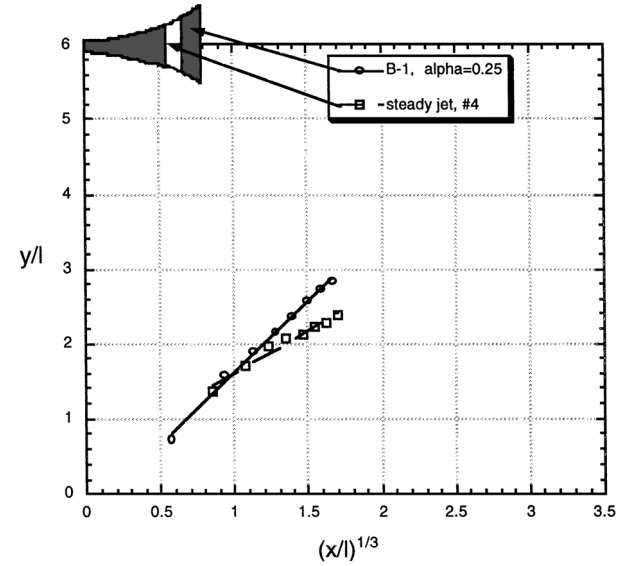

Fig. 11a Normalized penetration profiles of the exponential jet B-1 at α = 0.25 compared with a steady jet for equal thrust.

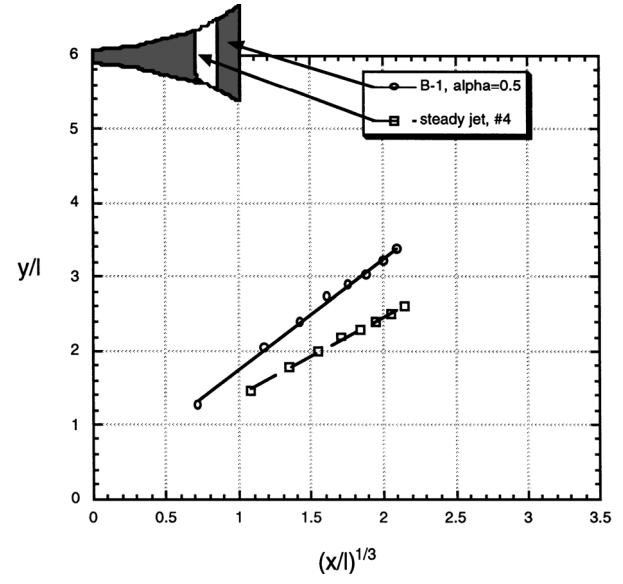

Fig. 11b Normalized penetration profiles of the exponential jet B-1 at α = 0.5 compared with a steady jet of equal thrust.

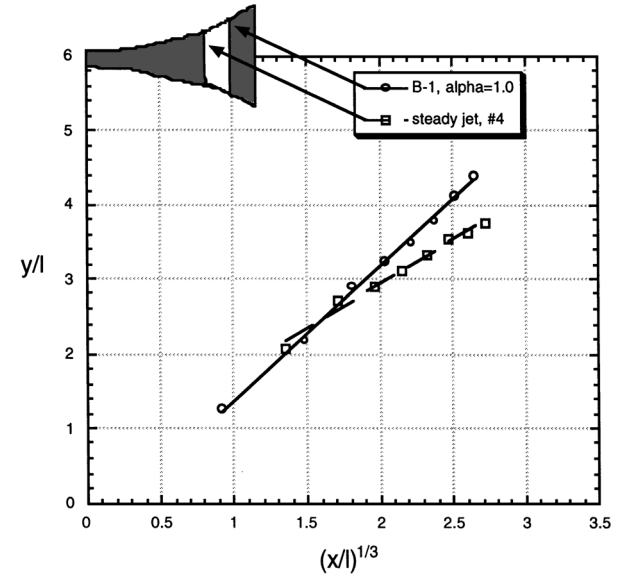

Fig. 11c Normalized penetration profiles of the exponential jet B-1 at α = 1.0 compared with a steady jet of equal thrust.

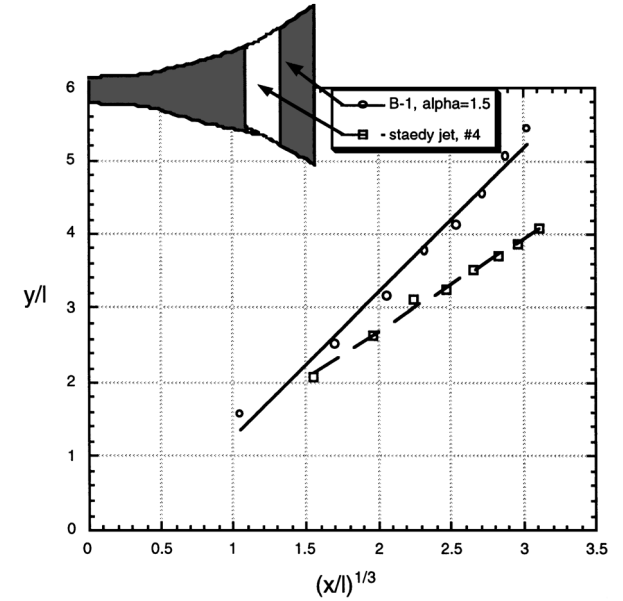

Fig. 11d Normalized penetration profiles of the exponential jet B-1 at α = 1.5 compared with a steady jet of equal thrust.

of α, the flame or reaction length decreases even as the vortex size is constant. According to experimental data by Fearn and Weston,[9] the strength of the vortex pair decreases as the jet-to-crossflow velocity ratio R decreases. Consequently, because $\alpha \approx 1/R$, increasing α means weaker vortices, thus less rapid mixing. However, the opposite is observed from Fig. 8, i.e., the flame or reaction length decreases with increasing α, indicating more rapid mixing.

Two factors can be given as possible explanations. The first one is that, although the visible size of the vortex pair does not change after $\alpha \cong 2.0$, the ability of the pair to incorporate pure jet fluid along the injection could decrease as it is convected below the injection region too fast, so that it would not make enough revolutions in the injection region. Thus, it is plausible to expect the jet to mix with the crossflow faster as α is increased beyond unity.

The second factor has to do with the shear layer ring vortices and the wake vortices replacing the counter-rotating vortex pair as the dominant structures in entrainment and mixing in this parameter range. This hypothesis is supported by the observations of the flow structure through flow visualization studies mentioned in the preceding section. In this parameter range, the physical appearance of the flow resembles a wake more than a transverse jet, with spanwise vortices being the main structures to be seen. Then one expects increased mixing or shorter flame or reaction lengths due to stronger wake vortices as the crossflow speed increases, because of the increasing momentum deficit in the wake region of the jet.

C. Penetration Depth

In a series of experiments, the transverse penetration depth of the exponential jet has been measured in an acceleration parameter range of $0.25 \leq \alpha \leq 1.5$ and compared with that of a single jet in crossflow. For this comparison, both the measured penetration depth y and streamwise distance x are normalized with a length scale l, which is defined[15] as

$$l = \left(\frac{T}{\rho_\infty U_\infty^2} \right)^{\frac{1}{2}}$$

where T is the total thrust imparted on the crossflow by the exponential jet as the sum of the thrusts of individual jets that make up the exponential jet, i.e.,

$$T = \sum_{i=1}^{n} \rho_i A_i V_i^2$$

The normalized penetration depth variation of exponential jet B-1 is given in Fig. 10 for all acceleration parameter values measured. It appears from these data that the far-field penetration depth of the exponential jet also obeys a $\frac{1}{3}$ power law as in the case of conventional transverse jets.

To investigate the effect of acceleration on the penetration of the jet, a series of comparison tests has been carried out with a single jet in crossflow. A logical choice of a single jet for this comparison is one of the five jets out of the exponential jet array to be operated at the same total thrust as the whole array. This was the fourth jet in the array, selected due to its geometry having an aspect ratio of about two, which is the closest to a conventional round jet among all five individual jets that make up the exponential array.

Normalized penetration measurements from these comparison tests are presented in Figs. 11a–11d, with a sketch of injector geometries of the same scale as axes. As can be seen from these data, in the near field, penetration of the exponential jet is comparable to or lower than those of the single jet. However, farther downstream, the exponential jet penetrates significantly deeper into the crossflow. At large values of the acceleration parameter range, the far-field penetration of the exponential jet exceeds those of the single jet by about 50%. Additionally, the slope of the penetration profile is clearly steeper in the case of the exponential jet. The results reported in Sec. VI are consistent with Refs. 25 and 26.

VII. Conclusions

Imposing an external timescale on the large-scale structure of a jet in a crossflow alters its entrainment and mixing characteristics significantly. The LIF tests revealed approximately a factor of three reductions in the size of a counter-rotating vortex pair as the acceleration parameter α is increased from 0.25 to 2.0. Meanwhile, the flame or reaction length, as measured with a chemical reaction in water, responds to acceleration also by increasing about 50% as α is increased from 0.5 to 1.0. Additionally, the far-field penetration of the exponential transverse jets exceeds the penetration of a conventional jet of equal thrust by about 40%.

It is evident from these data that acceleration provides a valuable tool, other than the jet-to-crossflow momentum ratio, to control mixing and penetration of a jet in a crossflow. Even though the concept of the accelerating transverse jet is new and requires further testing, the experiments reported here have shown that it may find important use in combustion and chemical processes where entrainment and mixing have significant effects on overall processes. These results are consistent with the careful and innovative observations of temporal jets accelerating into quiescent fluid by Zhang and Johari[25] and Johari and Paduano.[26]

Acknowledgments

This project was supported by the U.S. Air Force Office of Scientific Research under Grant AFOSR-87-0366. This support is gratefully acknowledged. A preliminary study with a temporally accelerating exponential jet by H. Li and R. E. Breidenthal has provided valuable results for the work reported here.

References

[1] Oster, D., and Wygnanski, I., "The Forced Mixing Layer Between Parallel Streams," *Journal of Fluid Mechanics*, Vol. 123, Oct. 1982, pp. 91–130.

[2] Roberts, F. A., "Effects of a Periodic Disturbance on Structure and Mixing in Turbulent Shear Flows and Wakes," Ph.D. Thesis, California Inst. of Technology, Pasadena, CA, 1985.

[3] Koch, C. R., Mungal, M. G., Reynolds, W. C., and Powell, J. D., "Helical Modes in Acoustically Excited Round Air Jet," *Physics of Fluids A*, Vol. 1, No. 9, 1989, p. 1443.

[4] Wu, J. M., Vakili, A. D., and Yu, F. M., "Investigation of the Interacting Flow of Nonsymmetric Jets in Crossflow," *AIAA Journal*, Vol. 26, No. 8, 1988, p. 940.

[5] Breidenthal, R. E., "Turbulent Mixing in Accelerating Jets," *Proceedings of the IUTAM Symposium* (Bangalore, India), Springer–Verlag, New York, 1987, pp. 459–470.

[6] Breidenthal, R. E., "The Turbulent Exponential Jet," *Physics of Fluids*, Vol. 29, No. 8, 1986, pp. 2346, 2347.

[7] Kato, S. M., Groenwegen, B. C., and Breidenthal, R. E., "On Turbulent Mixing in Nonsteady Jets," *AIAA Journal*, Vol. 25, No. 1, 1987, pp. 165–168.

[8] Clement, P., and Rodriguez, C., "Shock Wave Structure and Penetration Height in Transverse Jets," *AIAA Student Journal*, Vol. 27, No. 2, 1989, pp. 7–16.

[9] Fearn, R., and Weston, R. P., "Vorticity Associated with a Jet in a Cross Flow," *AIAA Journal*, Vol. 12, No. 12, 1974, pp. 1666–1671.

[10] Moussa, Z. M., Trischka, J. W., and Eskinazi, S., "The Near Field in the Mixing of a Round Jet with a Cross-Stream," *Journal of Fluid Mechanics*, Vol. 80, April 1977, pp. 49–80.

[11] Le Grivés, E., "Mixing Process Induced by the Vorticity Associated with the Penetration of a Jet into a Cross Flow," *Journal of Engineering for Power*, Vol. 100, July 1978, pp. 465–475.

[12] Keffer, J. F., and Baines, W. D., "The Round Turbulent Jet in a Cross-Wind," *Journal of Fluid Mechanics*, Vol. 15, April 1963, pp. 481–496.

[13] Savory, E., Toy, N., and Hossain, N., "An Experimental Study of the Potential Flow Parameters Associated with a Jet in a Crossflow," *AIAA/ASME/SIAM/APS 1st National Fluid Dynamics Congress, Collection of Technical Papers*, Pt. 2, AIAA, Washington, DC, 1988, pp. 932–939.

[14] Durando, N. A., "Vortices Induced in a Jet by a Subsonic Cross Flow," *AIAA Journal*, Vol. 9, No. 2, 1971, pp. 325–327.

[15] Broadwell, J. E., and Breidenthal, R. E., "Structure and Mixing of a Transverse Jet in Incompressible Flow," *Journal of Fluid Mechanics*, Vol. 148, Nov. 1984, pp. 405–412.

[16] Karagozian, A. R., "An Analytical Model for the Vorticity Associated with a Transverse Jet," *AIAA Journal*, Vol. 24, No. 3, 1986, pp. 429–434.

[17] Patankar, S. V., Basu, D. K., and Alpay, S. A., "Prediction of the Three-Dimensional Velocity Field of a Deflected Turbulent Jet," *Journal of Fluids Engineering*, Vol. 99, No. 4, 1977, pp. 758–762.

[18] Sykes, R. I., Lewellen, W. S., and Parker, S. F., "On the Vorticity Dynamics of a Turbulent Jet in a Crossflow," *Journal of Fluid Mechanics*, Vol. 168, July 1986, pp. 393–413.

[19] Coelho, S. L. V., and Hunt, J. C. R., "The Dynamics of the Near Field of Strong Jets in Crossflows," *Journal of Fluid Mechanics*, Vol. 200, March 1989, pp. 95–120.

[20]Johari, H., "An Experimental Investigation of Mixing in Buoyant Flows," Ph.D. Thesis, Dept. of Aeronautics and Astronautics, Univ. of Washington, Seattle, WA, 1989.

[21]Dahm, W. J. A., and Dimotakis, P. E., "Mixing at Large Schmidt Number in the Self-Similar Far Field of Turbulent Jets," *Journal of Fluid Mechanics*, Vol. 217, 1990, pp. 299–330.

[22]Dimotakis, P. E., and Brown, G. L., "The Mixing Layer at High Reynolds Number: Large Structure Dynamics and Entrainment," *Journal of Fluid Mechanics*, Vol. 78, Dec. 1976, pp. 535–560.

[23]Broadwell, J. E., and Breidenthal, R. E., "A Simple Model of Mixing and Chemical Reaction in a Turbulent Shear Layer," *Journal of Fluid Mechanics*, Vol. 125, Dec. 1982, pp. 397–410.

[24]Gharib, M., "The Effect of Flow Oscillations on Cavity Drag and a Technique for Their Control," Ph.D. Thesis, California Inst. of Technology, Pasadena, CA, 1983.

[25]Zhang, Q., and Johari, H., "Effects of Acceleration on Turbulent Jets," *Physics of Fluids*, Vol. 8, No. 8, 1996, pp. 2185–2195.

[26]Johari, H., and Paduano, R., "Dilution and Mixing in an Unsteady Turbulent Jet," *Experiments in Fluids*, Vol. 23, No. 4, 1997, pp. 272–280.

G. M. Faeth
Editor-in-Chief